Quantifying Myofascial Dysfunction in Post-Stroke Pain

NCT05762679

7/28/2023

JHM IRB - eForm A – Protocol

- **Use the section headings to write the JHM IRB eForm A, inserting the appropriate material in each. If a section is not applicable, leave heading in and insert N/A.**
- **When submitting JHM IRB eForm A (new or revised), enter the date submitted to the field at the top of JHM IRB eForm A.**

****

1. Abstract

a. **Provide no more than a one page research abstract briefly stating the problem, the research hypothesis, and the importance of the research.**

Shoulder pain is extremely common after stroke and occurs in 30-70% of patients [1, 2]. The pain may begin as early as one week after stroke [3], although peak onset and severity occurs around four months [4, 5], and persists into the chronic stage [6, 7]. Chronic post stroke shoulder pain (PSSP) interferes with motor recovery, decreases quality of life, and contributes to depression [5, 8, 9]. PSSP is thought to be caused mainly by damage to the myofascial tissues around the shoulder joint [10-12]. Interestingly, an MRI study in patients with PSSP showed that the degree of structural damage to the muscles did not correlate with the degree of pain [13]. ***Thus, the pathophysiology of myofascial dysfunction and pain in PSSP has not been elucidated leading to missed opportunities for early diagnosis and variable success with pain management.***

The accumulation of hyaluronic acid (HA) in muscle and its fascia can cause myofascial dysfunction [14]. HA is a glycosaminoglycan (GAG) consisting of long-chain polymers of disaccharide units of glucuronic acid and N-acetylglucosamine and is a chief constituent of the extracellular matrix of muscle [15]. In physiologic quantities, HA functions as a lubricant and a viscoelastic shock absorber [16], enabling force transmission during contraction and stretch [17]. Reduced joint mobility [18] and spasticity [19] result in focal accumulation and alteration of HA in muscle. This can lead to the development of stiff areas and taut bands, dysfunctional gliding of deep fascia and muscle layers, reduced range of motion (ROM), and pain [20]. ***However, the association of muscle HA accumulation with PSSP has not been established.***

We have quantified the concentration of HA in muscle using T1rho (T1ρ) MRI and found that T1ρ relaxation time is increased in post stroke muscle stiffness [21-23]. Since HA is highly hydrophilic, HA-rich taut bands are hypoechogenic on grey-scale ultrasound (US) [24, 25], making it possible to develop a clinic-friendly quantitative US tool to infer the abnormal accumulation of HA. Furthermore, dynamic US imaging using shear strain mapping can quantify dysfunctional gliding of muscle that may generate pain during ROM [26]. Myofascial dysfunction can result in non-painful reduction in ROM (latent PSSP), which may become painful due to episodic overuse injury producing greater shear dysfunction (active PSSP). Hence, shear strain mapping may differentiate between latent versus active PSSP. ***Thus, quantitative MR and US imaging may serve as useful biomarkers to elucidate the pathophysiology of myofascial dysfunction.***

IMPACT

This proposal will develop quantitative imaging biomarkers of myofascial dysfunction in PSSP and assess their ability to monitor response to treatment. It aligns with the NIH HEAL Initiative to bolster research to improve treatment and enhance pain management.

2. Objectives (include all primary and secondary objectives)

AIM 1. Quantify the extent of HA accumulation in shoulder muscles using quantitative MRI and US.

Research Hypothesis: Patients with PSSP will show increased T1ρ relaxation times in the paretic compared with the non-paretic muscles, which will correlate with a distinct echo texture pattern on US.

AIM 2. Distinguish between latent versus active PSSP using US shear strain mapping in the paretic compared with the non-paretic muscles.

Research Hypothesis: Shear strain will be lowest in active PSSP compared with latent PSSP, relative to the non-paretic side.

3. Background (briefly describe pre-clinical and clinical data, current experience with procedures, drug or device, and any other relevant information to justify the research)

Contribution of Myofascial Dysfunction to PSSP. A large proportion of post-stroke pain is musculoskeletal, with shoulder pain contributing the largest fraction [27]. The human shoulder is a complex shallow ball-and-socket joint, and its multidirectional mobility is highly dependent on the coordinated action of several muscles shown in **Figure 1A.** A key characteristic of shoulder movement is the scapulohumeral rhythm which is the ratio of glenohumeral motion to scapulothoracic motion during humeral elevation (**Figure 1B**) [28]. The scapulohumeral rhythm is disrupted after stroke due to a combination of impaired strength, increased tone,

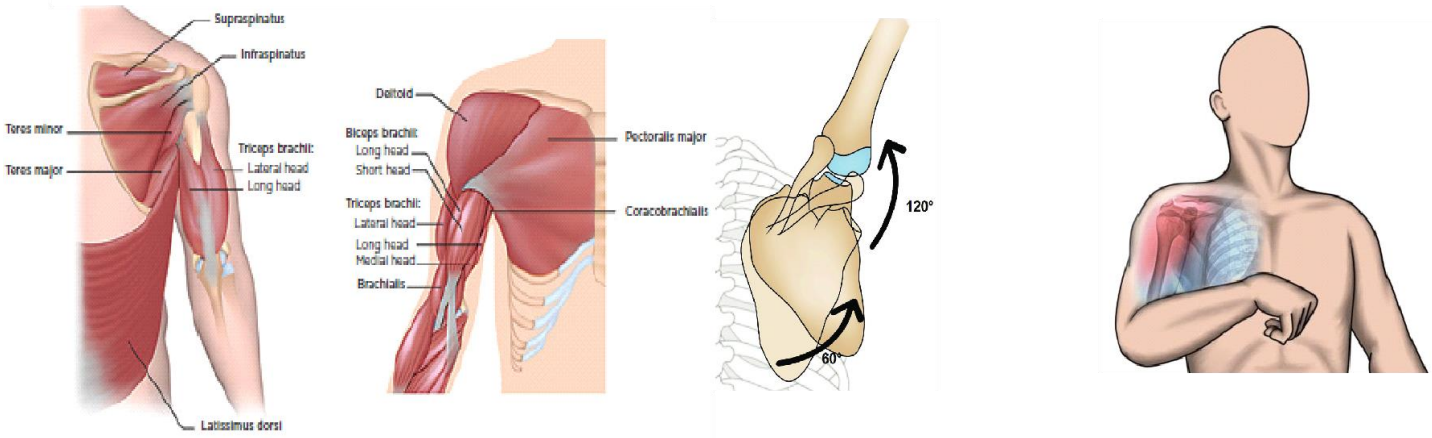

Figure 1. Shoulder girdle and arm muscles (A) largely responsible for the scapulohumeral rhythm (B). Characteristic posture with increased shoulder internal rotation during attempted arm elevation causing shoulder pain after stroke (C).

incoordination due to aberrant muscle recruitment, and fatigue [10], leading to reduced humeral elevation and scapular upward rotation and increased scapular internal rotation during arm elevation [29, 30], which predispose to shoulder pain [31] (**Figure 1C**).

Studies have reported that 85% of patients with spastic hemiplegia experience pain compared with 18% of those with flaccid hemiplegia [32]. Muscle shortening and decreased ROM associated with spasticity and muscle stiffness can exert tension on the muscles and cause pain during stretching. Reduced shoulder ER is strongly correlated with shoulder pain [33-35], which if left untreated can result in painful contracture of the shoulder [36]. Restricted muscle ROM, in turn, can increase the risk of muscle injury, nerve impingements and produce excessive shear and compressive joint forces that may also contribute to shoulder pain [13, 37, 38]. Despite the known involvement of the muscles in shoulder pain, the pathophysiology of myofascial dysfunction is unclear, which impedes both prevention and effective treatment of PSSP.

Intramuscular HA and its Contribution to Myofascial Dysfunction. Even in the absence of any active force generation, the non-contractile elastic elements in muscle generate passive forces when stretched [39]. The endomysium, perimysium and epimysium collectively form the extracellular matrix (ECM) of muscle and are composed of collagens and elastic fibers embedded in a viscoelastic gel of proteoglycans, glycoproteins, and glycosaminoglycans (GAGs) such as HA. When the myofibrillar proteins and proteoglycans are removed, the honeycombed 3-D network of the collagenous connective tissue can be seen [40-42] (**Figure 2A**). When a muscle fiber contracts or is stretched, the preferred orientation of the collagen fibers in the endomysium changes accounting for the non-linear increase in passive resistance and leads to trans-laminar shear during force transmission through the ECM [42, 43]. HA is the most abundant molecule in the ECM – it is present around the endomysium of individual muscle fibers and in the perimysium and epimysium of human muscle [44] (**Figure 2B**). The perimysium and epimysium define slip planes between muscle fascicles and whole muscles, enabling them to slide past each other during stretch and contraction, causing large shear displacements and shape changes in the whole muscle [17]. The shear forces across adjacent muscle fibers, muscle bundles and whole muscles are strongly determined by the composition and viscoelastic properties of the proteoglycan matrix of the ECM, specifically of HA.

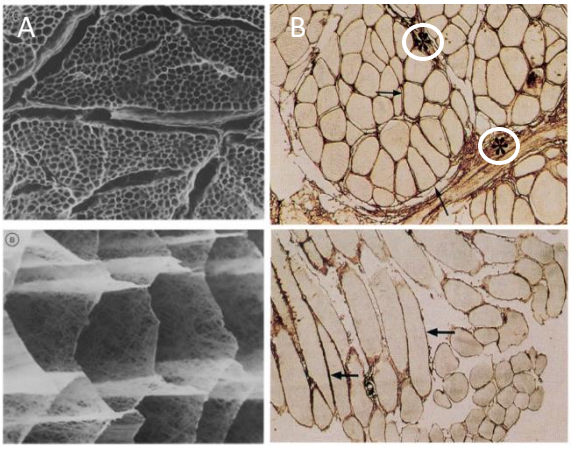

Figure 2. Scanning electron micrographs of muscle after removal of myofibrillar proteins and proteoglycans showing the honeycombed ECM (A). Note brown staining of HA with HA binding protein adjacent to the endomysium (arrows) and especially in the perimysium (* in white circles) (B).

HA has been traditionally regarded as a space-filling ground substance [44, 45]. It is the only non-sulfated GAG composed of a repeating disaccharide of glucuronic acid and N-acetyl glucosamine that forms long chains or polymers assuming molecular weights of the order of 10^5 to 10^7 Da and an extended length of 0.25–25 μm [46]. The chemical structure of HA makes it highly hydrophilic, enabling the molecule to retain water and swell. However, as the concentration and molecular weight of HA increases, it entrains more water and the viscosity of the solution increases exponentially [47, 48] (**Figure 3A**); *a 10 mg/ml solution of 1.5 x 10^6 Da HA has a viscosity 5000x that of water.* The molecular weight and viscosity of HA solutions affects tissue lubrication, hydration, and the physical stiffness of the tissues [49]. HA shows non-linear viscoelastic behavior [50-54], implying that a muscle with higher HA concentrations, and hence higher viscoelasticity will show greater passive resistance to stretch or contraction. Thus, the concentration and rheological properties of the HA in the ECM of muscle can contribute significantly to increased passive resistance during movement [55, 56], which may produce myofascial dysfunction.

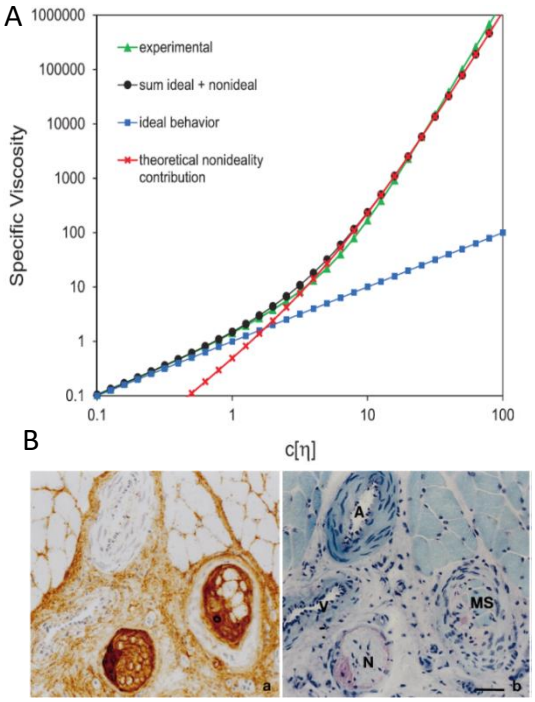

Figure 3. HA in physiological saline (experimental), shows marked increase in viscosity with increasing concentration – nonideal behavior (A). Muscle spindles (MS) and the perineural areas (N) are abundant in HA (brown stained) (B). The two sides show the same structures that are stained differently.

Muscle spindle receptors and nerve fibers, responsible for sensing and responding to stretch, reside within the HA-rich perimysium, and are also abundant in HA [57] (**Figure 3B**). The axial and periaxial spaces of the muscle spindles, all layers of the spindle capsule, as well as the endoneurium in the space between individual axons are rich in HA. The presence of HA in the periaxial fluid has been shown to be responsible for the transcapsular potential which increases the sensitivity of the sensory endings to mechanical stimuli [58]. Alteration in the viscosity of the HA solution in the muscle spindle and around the nerve endings can thus increase the sensitivity of the muscle spindles and nerves to stretch [59, 60], potentially causing dysesthesia and pain.

Imaging HA Accumulation in Stroke and Myofascial Dysfunction using MRI. We proposed the hyaluronan hypothesis of muscle stiffness, which postulated that the deposition of HA in the ECM of muscle contributes to the development of muscle stiffness by dramatically altering its viscosity [19, 25]. This hypothesis was informed by a study where the ankle joint in rats was immobilized, which resulted in increased muscle HA content and muscle shortening 4 weeks post-immobilization compared to controls [18]. However, thickening and disorganization of endomysial collagen fibrils only became apparent by 12 weeks post immobilization. In a proof-of-concept study to determine if patients with post-stroke arm immobility and muscle stiffness also show increased HA accumulation, we performed T1ρ MRI to quantify the T1ρ relaxation time in the upper arm muscles of patients post stroke compared to healthy controls [61] (**Figure 4**). Note that the T1ρ relaxation time is non-uniformly increased in the muscle, with perhaps

more accumulation in the perimysium, between the muscle fascicles. This may have caused an alteration in the shape of the muscles post stroke [17], which appear to be stuck together, giving the upper arm a triangular shape compared to controls. While the T1ρ MRI is not specific for HA, HA is the most abundant GAG, and subsequent studies showed that it can be reduced with the enzyme hyaluronidase (see **Section A.5**), suggesting that HA is responsible for the signal.

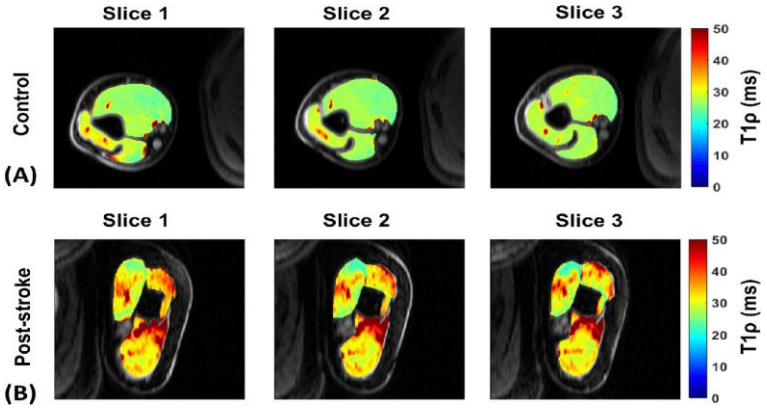

Figure 4. Quantification of GAG in muscle using T1rho (T1ρ) MRI. Note increased intramuscular T1ρ relaxation times (more red) in patients with post stroke muscle stiffness compared to controls.

Interestingly, histological studies in animal models of overuse injury also show increased levels of HA in the ***epimysium*** of the overused muscle - HA concentration increased 2.8-fold after 2 days of overuse and remained significantly increased at 7 days, and then decreased gradually towards control levels by 14 days [62]. Overuse injury causing myofascial pain in humans has also been associated with HA accumulation [14]. The formation of taut bands that constitute trigger points is attributed to increased viscosity from focal accumulation of high molecular weight chains of HA [24]. This can result in dysfunctional gliding of deep fascia and muscle layers, forming the basis of myofascial pain [20]. We published a recent case series of patients with non-traumatic chronic myofascial pain in the lateral aspect of the elbow who showed imaging evidence of abnormally elevated GAGs using T1ρ MRI [21] (**Figure 5**, PRE). Note that this ***accumulation is primarily in the epimysium and in the extra-muscular fascia***, and decreased after fascial manipulation treatment (**Figure 5**, POST). This data is consistent with the data from animal models of overuse injury [62], and suggests that HA synthesis is stimulated by muscle overuse, but it may not be a problem unless the stimulus persists, or is followed by immobility, for example due to paresis from a stroke. Exercise in healthy individuals has been shown to increase serum HA significantly, but the serum levels decrease rapidly to lower than resting levels by 30 min post exercise [44], suggesting that movement mobilizes HA from muscle into the circulation, which is cleared rapidly. Conversely, lack of movement, for example, overnight, can lead to morning stiffness which improves as HA is mechanically driven out into the circulation by physical activity upon awakening [63]. Taken together, these studies demonstrate that both immobility and muscle overuse can lead to HA accumulation in muscle and imaged using T1ρ MRI.

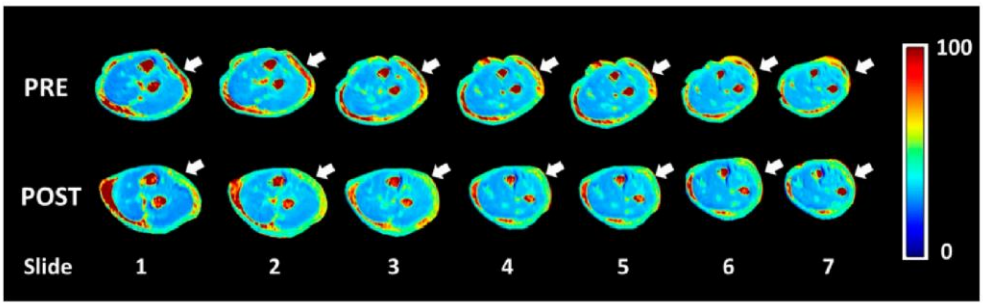

Figure 5. Quantification of GAG using T1rho (T1ρ) MRI in myofascial pain. Note increased T1ρ relaxation times (red) in the extra-muscular fascia in patients with lateral elbow pain (pre, arrows) and its reduction after fascial manipulation (post, arrows).

US is more accessible than MRI for clinical imaging [64]. Healthy muscles look dark with sharp bright lines on grey-scale US. The dark signal is hypoechoic and the bright lines represent hyperechoic signal from collagen fibers in the endomysium and perimysium. The echogenicity of muscle tissue can describe alterations in the structure of muscles. Trigger points, which are stiff nodules in a taut band of muscle, present a hypoechoic signal [65, 66], which can be explained by the fact that HA is hydrophilic, and areas of HA accumulation entrain more water and become highly viscous [47, 48]. Increased ECM viscosity leads to "densification" or increased stiffness of the tissue [67]. Qualitative assessment of muscle echo, however, cannot provide an accurate measure of tissue properties [68]. Recently, quantitative US has emerged where the envelope statistics of the radiofrequency components of the backscattered US signal can be used to objectively differentiate tissue properties [69]. US scattering occurs primarily at interfaces, such as connective tissues of the endomysium, perimysium, and fascia and other components, including muscle cells, fat, and fibrous tissue; the mismatch of acoustic impedance can be quantified to provide echo texture maps to characterize tissue properties [70, 71], and statistical maps of muscle echo texture can be used to diagnose myofascial dysfunction [72]. **Thus Aim 1 will quantify the extent of HA accumulation in paretic shoulder muscles compared with the non-paretic side in patients with PSSP using T1ρ MRI, and secondarily correlate the T1ρ MRI measures with US echo texture to develop a clinic-friendly tool to infer extent of HA accumulation**.

Imaging Myofascial Dysfunction and Differentiating Latent and Active Pain Using Quantitative US. The relationship of abnormal HA accumulation in muscle to pain is likely to be dependent on muscle use. An MRI study of 89 patients with chronic PSSP showed that 35% of subjects exhibited a tear, and 53% of subjects exhibited tendinopathy of at least one rotator cuff, biceps or deltoid muscle. However, the tears and tendinopathies were not related to the severity of PSSP; instead, the degree of muscle atrophy was related to reduced severity of PSSP [13]. Since patients with PSSP also have greater motor impairment [12], they are likely to move it less, leading to more atrophy, and less pain. A study of the incidence and prevalence of PSSP among different regions of the world suggests that it is more prevalent in regions that offer more rehabilitation, suggesting that PSSP may be triggered by microtrauma during movement [73]. A stiff, shortened muscle is more likely to resist stretch, and become injured and inflamed during use. Shoulder pain during movement, especially during shoulder ER after stroke, predicts long term shoulder pain [74], suggesting that active PSSP is perhaps provoked by overuse of already dysfunctional, stiff shoulder muscles, making it distinguishable from latent PSSP.

Strain is the most commonly encountered muscle injury and characteristically occurs at the musculotendinous junction, where maximal stress accumulates, especially during eccentric (stretching) exercise [75]. The epimysium is continuous with the musculotendinous junction [76], and overuse injury is associated with accumulation of HA in the epimysium [21]. Since alteration in the viscoelastic properties of the accumulated HA can dramatically alter the shear plane motion [17], post-stroke muscle stiffness overlaid by overuse injury may cause greater shear dysfunction. However, the shear dysfunction and strain injury from microtrauma or overuse injury may not be detected using routine MRI or US [77, 78]. Shear strain can be quantified by US shear strain mapping -- a computational technique where a series of ultrasound images are acquired in rapid succession and cross correlation methods are used to quantify the relative mobility of layers within inter- and intramuscular fascia during motion [26]. Using this

technique, it was found that shear strain was reduced by 20% in the thoracolumbar fascia during passive movement in individuals with low back pain versus those without low back pain. Hence it is possible that quantification of shear strain will be able to distinguish between latent and active PSSP compared with the healthy state. **Thus Aim 2 will distinguish between latent versus active PSSP using US shear strain mapping during passive shoulder ER in the paretic shoulder muscles compared with the non-paretic side.**

INNOVATION

This proposal is innovative in several ways:

MR/US Imaging Innovation: T1ρ relaxation mapping of muscle will quantify GAG content in muscle non-invasively. Direct methods using muscle biopsy and staining for HA are not ethical or practical to perform before and after injections in humans. Our research team has shown that it is feasible to use 3D-T1ρ to map GAG content in muscle in patients with stroke and myofascial dysfunction non-invasively [21-23], without the use of exogenous contrast agent injection or radiofrequency hardware modifications. In addition, we will correlate T1ρ relaxation times with statistical echo texture maps obtained using quantitative US to develop a clinic-friendly tool to infer extent of HA accumulation. These innovations will establish the pathophysiology of myofascial dysfunction in PSSP to enable appropriate treatment and monitoring.

Quantitative US Innovation 2: Shear strain mapping has the potential to differentiate between latent pain and active pain in PSSP. Movement restriction reduces shear strain measured using quantitative US in a porcine model of back pain. However, the combination of movement restriction and local injury leads to an additive, and quantifiable reduction in US shear strain [79], suggesting that US shear strain mapping may be able to differentiate latent PSSP (due to movement restriction alone) from active PSSP (due to a combination of movement restriction and local injury). Using this method in PSSP will enable the quantification of the underlying pathophysiology that leads to latent and active PSSP. This will enhance pain management to address the underlying pathophysiology rather than just provide symptomatic relief.

Approach Innovation: We will use the Bimanual Arm Trainer (BAT) to provide passive shoulder ER and assess pain-free shoulder ER. Several studies show a strong association between shoulder immobility and non-use, stiffness in the pectoralis major muscle, limitation in shoulder ER and PSSP [33-35] (**Figure 6**). We will use the BAT – an FDA-cleared device designed specifically to provide gentle, controlled passive ER-ROM (unimanual mode) at a fixed rate during shear strain mapping. For precise quantification of pain-free passive ER-ROM before and after treatment in the clinical trial, patients will use the non-paretic limb as the actuator (bimanual mode) enabling safe movements that are patient-controlled [80].

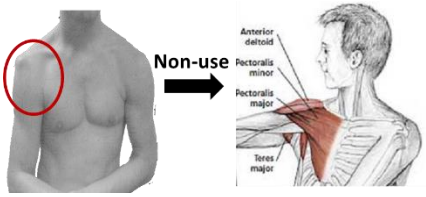

Figure 6. Immobility and non-use of the paretic upper limb leads to stiffness and shortening in the pectoralis major muscle, limiting shoulder ER-ROM.

APPROACH

Overview: The primary objective of the R61 phase is to identify and develop quantitative measures that can differentiate abnormal myofascial tissues in latent versus active PSSP from relatively healthy tissues on the non-paretic side along with cross-sectional correlations with

clinical signs and symptoms. In addition, we will build the team to plan the R33 phase clinical trial during this first phase.

Definition of latent PSSP: The latent phase includes myofascial dysfunction, including soft tissue stiffness and non-painful reduction in ROM, which may be accompanied by focal palpable nodules that are tender to palpation. ***We will define latent PSSP as a difference of more than 10 degrees of passive ER-ROM between the non-paretic and paretic shoulders, with focal palpable nodules that may be tender on palpation with pain rating of <5/10*** [81].

Definition of active PSSP: During the active phase, the patient has painful reduction in ROM, spontaneous pain, and localized, tender indurated nodules on palpation of muscles that reproduces the local and/or radiating pain. Rajaratnam et al. found that a positive Neer test, which elicits pain on passive forward elevation of the arm with the scapula stabilized (**Figure 7A**), combined with the hand-behind-neck (HBN) maneuver eliciting a pain rating of ≥ 5/10 (**Figure 7B**), and a difference of more than 10 degrees of passive ER-ROM between the non-paretic and paretic shoulders has a 98% probability of predicting PSSP with 96.7% sensitivity and 99.0% specificity [81]. ***We will define active PSSP as a difference of more than 10 degrees of passive ER-ROM between the non-paretic and paretic shoulders, with focal palpable nodules that are tender on palpation, reproducing the pain, and eliciting a pain rating of ≥5/10 when combined with the HBN maneuver.***

Figure 7. Depiction of Neer test (A) and Hand-behind-neck (HBN) test (B) used to diagnose active PSSP (8).

4. Study Procedures

a. Study design, including the sequence and timing of study procedures (distinguish research procedures from those that are part of routine care).

All procedures will be conducted solely for study purposes. We will conduct a cross-sectional observational study in 40 patients for the R61 phase. 20 patients will have latent PSSP with non-painful restriction in passive shoulder ER-ROM in their paretic arm, and 20 will have active PSSP with painful (≥ 5/10) restriction in passive shoulder ER-ROM as defined above. All 40 subjects will also undergo testing on their non-paretic arm which will serve as a proxy for "healthy" control. All subjects will undergo ***3 types of quantitative imaging of the pectoralis major (key internal rotator) and infraspinatus (key external rotator) muscles of both arms:*** (1) 3-D T1ρ MRI to quantify the extent of HA accumulation (primary outcome for Aim 1), (2) Quantitative US statistical echo texture mapping (secondary outcome for Aim 1), and (3) Quantitative US shear strain mapping to distinguish between latent and active PSSP on the paretic side compared with the non-paretic side (primary outcome for Aim 2).

After obtaining informed consent, subjects will be screened to ensure that they meet inclusion-exclusion criteria. They will then undergo the following clinical and imaging assessments.

Clinical Assessments: All clinical assessments will be performed on both arms and be used to correlate with the imaging measures.

Passive ROM in the upper limb will be measured at the shoulder (flexion-extension, abduction-adduction, internal and external rotation) in the standard sagittal, horizontal and coronal planes using video and/or 3-D motion capture techniques (Motion Monitor, Innovative Sports Training, Inc., Chicago, IL) [82]. This system uses the trackSTAR 800 sensor (Ascension Technology Corp., VT) that has a static resolution of 0.5 mm for position and 0.1° for angular orientation [83]. During passive ROM, we will also assess muscle stiffness with the Modified Ashworth Scale [84] to determine the degree of resistance [85].

Shoulder pain characteristics will be measured by assessing shoulder pain onset, pain location, pain during movements and/or at rest, pain at touch, pain intensity, pain quality and intake of medication for the shoulder pain. The pain quality will be assessed as dull ache, stabbing/ cutting, scurrying/radiating, burning, muscle cramps or tiredness, or described by the patient. Sensory testing for light touch will be assessed using a cotton swab in the upper arm and forearm, hands and fingers, and recorded as normal, diminished, increased or absent. Hypoesthesia (decreased sensitivity to tactile stimulation), Hypoalgesia (diminished pain in response to a normally painful stimulus), Hyperesthesia (increased sensitivity to tactile stimulation), Dysesthesia (an unpleasant abnormal sensation, whether spontaneous or evoked), and Allodynia (pain due to a stimulus that does not normally provoke pain) will be defined as per the taxonomy of the International Association for the Study of Pain (IASP) [86]. We will assess for vasomotor changes such as limb edema and color, and alterations in skin temperature between the paretic and non-paretic limbs due to local hyperactivity of the sympathetic nervous system [89, 90]. We will also assess local stiffness, using the stiffness rating scale [24] and the Pact sense muscle scanner which quantifies “haptic feeling” or what the muscle feels like when probed with the hand (https://www.thepact.com/technology). The Pact sense quantifies stiffness, measured in units of [N/m] and damping, measured in units of [Ns/m], as well as their slopes, and the symmetry across the measurements of the two sides of the body. The measurement process is purely mechanical and non-invasive, and includes no optical, electrical, or chemical interactions with the skin or muscles. In addition, we will measure pressure sensitivity thresholds using an algometer and rate the pain elicited on a pain rating scale.

Upper limb motor impairment will be measured using the upper limb Fugl-Meyer Scale (FMS) [91], a validated, widely used, standard scale of motor impairment post-stroke. It consists of 33 tasks, each is scored on a 3-point scale (0 unable to perform, 1 partially perform, 2 faultless performance); the maximum score for the upper extremity is 66. The FMS score reflects the degree to which joint movements can be isolated.

Upper limb function will be measured with the Wolf motor function test (WMFT) [92], a battery of functional tasks that are timed and scored on movement quality. We will use the streamlined version, which has six tasks [93], and has been validated for use in the subacute stage post-stroke [94].

Stroke-specific quality of life will be measured using the Stroke Impact Scale [95, 96], a self-reported health status measure that assesses multidimensional stroke outcomes in eight domains: strength, hand function, mobility, activities of daily living, emotion, memory, communication, and social participation. Additionally we will assess depression using the PHQ-2, as pain and depression are strongly associated [97].

HEAL core pain clinical patient reported outcomes: The following pain-related patient-reported outcomes will be collected-- Pain, Enjoyment of life and General Activity (PEG) scale, PROMIS Physical Function Short Form 6b, PROMIS Sleep Disturbance form 6a and sleep duration question, Pain Catastrophizing Scale Short Form 6, Patient Health Questinnaire-2, Generalized

Anxiety Disorder-2, Patients' Global Impressions of Change (PGIC) scale, and the Tool's First-Stage Screening Component (TAPS-1).

Imaging Assessments: All imaging assessments will be performed on both arms.

Aim 1: Quantify the extent of HA accumulation in shoulder muscles using quantitative MRI and US.

(a) T1ρ MRI: All images will be acquired using a 3T Prisma whole-body MRI scanner (Siemens Healthcare, Erlangen, Germany) in the Nelson/Harvey building, employing a body coil (Tx)/ flex wrap receive array coil with 8 coil-elements over the pectoralis major and infraspinatus muscles. Anatomical muscle MR images (proton density, T1-w and T2-W) will be acquired using 2D-FSE sequences. A 3D-turbo-FLASH (fast, low angle shot) MRI sequence with a customized T1ρ preparation module will be used to enable varying spin lock durations (TSL). A paired self-compensated spin-lock pulse will be used to minimize B0 and B1 variations [98]. The sequence parameters will include FOV = 130 mm, matrix size = 256 × 64 × 64, TR = 1500 ms, resolution = 0.5 × 2 × 2 mm2, spin-lock frequency = 500 Hz, 10 TSL durations = 2, 4, 6, 8, 10, 15, 25, 35, 45, 55 ms. acquisition duration = ~18 minutes for each arm. The MRI body coil will be used for transmission, and vendor supplied flexible receive array coils (8 coil elements each) will be used to image the non-paretic and paretic sides in all subjects. To investigate the extent to which fatty infiltration in skeletal muscle plays a role, Dixon based methods will be used to separate fat and water distribution using the iterative decomposition of water and fat with echo asymmetry and least-squares estimation (IDEAL) technique [99, 100]. The Dixon water/fat imaging parameters will include TR = 9.3 ms, TE = (2.26, 3.08, 3.90) ms, FOV = 180 mm, matrix size = 128 × 128, resolution = 1.4 × 1.4 mm2, total acquisition time ~ 4.5 min for each arm. Total scan time for both arms will not exceed 90 min.

MRI Data Processing: Manual ROIs will be drawn for the pectoralis major and infraspinatus muscles. The mono-exponential T1ρ mapping will be performed by fitting the signal intensity at different spin-lock durations for each pixel using a three-parameter non-linear mono-exponential model (**Equation 1**) where S is the signal intensity, A is the amplitude, TSL is the spin lock duration, T1ρ is the mono-exponential relaxation time in the rotating frame, and A0 is the average noise level [22, 23]. For the Dixon water-fat imaging, IDEAL post-processing will be used to separate the water and fat images from the 3-echo images. Water-fractions and fat-fractions will be calculated from the water and fat images. The fat-fraction maps will be used to quantify fat infiltration in the muscles.

Equation 1

$$S = A \cdot e^{-TSL/T_{1\rho}} + A_0$$

MRI Data Analysis: The mean values and standard deviations of T1ρ relaxation times (ms) will be obtained from the defined regions of interest in the pectoralis major and infraspinatus muscles and will be compared on the paretic and non-paretic sides using mixed model analysis wherein the two sides are nested within one person, and healthy (non-paretic) versus latent PSSP versus active PSSP are examined as fixed effects. Prior to final analysis we will perform model diagnostics to assure that model assumptions regarding the fixed and random effects are met. The mean water and fat fractions of the muscles will also be obtained in percentages to quantify fat infiltration in the muscles, which will be used as predictors in the analysis. We will use Pearson's correlations to correlate the clinical and imaging measures.

Expected results, potential pitfalls & solutions: We expect an increase in T1ρ relaxation times in the paretic pectoralis major and infraspinatus muscles compared with the non-paretic side. We may also see a difference in location of the signal and/or relaxation times between latent and active PSSP. For example, subjects with active PSSP may show higher relaxation times in the

epimysial regions as seen with overuse injury, whereas subjects with latent PSSP may show higher relaxation times in the perimysial region. A two-compartment model of T1ρ mapping (bi-exponential model) can separate out the signal from the GAG content and the free water content of the ECM, and delineate a clearer picture of the extracellular environment of the muscle [23]. We can also analyze the data collected using this model, which may differentiate latent form active PSSP.

All the MRI data will be collected and analyzed in collaboration with co-I Dr. Laura Fayad at Johns Hopkins in conjunction with Dr. Rajiv Menon at NYU Langone.

(b) US Echo Texture Mapping: Ultrasound imaging will be performed with an Alpinion E-CUBE12R US system (Seoul, South Korea) equipped with an L8-17 transducer with a frequency range of 8 to 17 MHz and a 20-mm width or the Clarius C3 Scanner HD (Vancouver, Canada) in the Motor Recovery Research Lab. The participant will be seated comfortably with the arm supported on an arm rest. The skin surface over the pectoralis major muscle will be marked with the muscle relaxed. All images were acquired with the same US system settings. The musculoskeletal imaging preset will be used with a 10-MHz center frequency, 3-cm depth, and 76-dB dynamic range. The pectoralis major muscle will be visualized in cross section at the location of the skin mark, and images will be acquired with the muscle relaxed, with the US transducer held steadily at the same anatomic location, in a direction perpendicular to the skin surface. Raw RF US data will be saved at a sampling frequency of 40 mega-samples/s.

US Data Processing: The intensity of the raw RF US data will be calculated using the Hilbert transform. For each participant, a single B-mode image frame at rest will be selected. Two different types of analyses will be performed. First, we will create spatial parameter maps by estimating the statistical model parameters from the histogram of echo intensities within a moving rectangular window. The window size will be varied from 3 times the acoustic wavelength to 7 times the wavelength. Second, we will select the entire muscle as the ROI for estimating the model parameters. For this analysis, the muscle will be identified manually in the corresponding B-mode images, and the muscle boundary will be manually marked by identifying the hyperechoic fascia boundaries. The entire muscle will be considered the ROI for analysis, including all fascia interfaces inside the muscle boundaries. The backscattered intensities within this muscle ROI will be normalized by the maximum value within the ROI and analyzed as per the theoretical models described in [69].

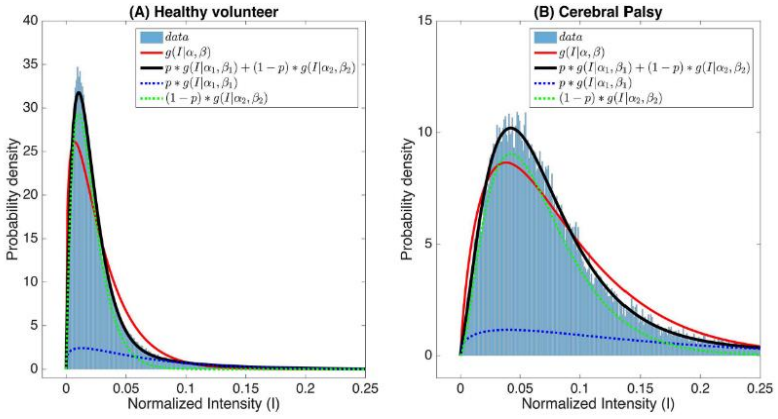

Figure 8. Histogram of backscattered US intensities in a healthy volunteer and in a patient with cerebral palsy.

US Data Analysis: The model parameters (signal to noise ratio (SNR), shape and rate of the single gamma distribution, and shape, rate, and mixture probability of the gamma distributions (for example, **Figure 8**) will be estimated from the muscle images at rest in the non-paretic and paretic pectoralis major and infraspinatus muscles. We will use the SNR parameters to investigate the deviation from purely diffuse scattering. We will then investigate whether the gamma distributions are a good fit to the underlying data using descriptive statistics and the Chi-square goodness-of-fit statistic. The estimated parameters will be compared between the non-paretic and paretic sides. Log transformations will be applied to

the rate parameters to approximate normality. Pearson's r will also be used to assess the correlation between the T1ρ relaxation times, and the shape and rate parameters of the gamma distributions with sufficiently high signal to noise ratio (SNR) obtained from the statistical echo texture maps US.

Expected results, potential pitfalls & solutions: We expect that at least one of the shape and/ or rate parameters for a mixture of two gamma distributions from the backscattered echo intensity of the muscles will correlate strongly with the T1ρ relaxation times. If so, this will provide a quantitative clinic-friendly tool to infer the GAG/HA accumulation in the muscle, which will enable treatment monitoring. A limitation of using a mixture of gamma distributions is that the quantitative US model parameters cannot directly be linked to some tissue characteristics such as the effective scatterer size or coherent scatterer power, which may be possible with the use of more sophisticated model fits such as the homodyne K distribution. However, the parameters of the gamma distribution do relate to tissue characteristics that affect coherent and diffuse scattering, and changes in the parameters are directly related to changes in the tissue composition and microarchitecture. One advantage of using the mixture of gamma distributions is that the parameter estimation can be performed robustly by using well-established approaches.

Aim 2: Distinguish between latent versus active PSSP using US shear strain mapping in the paretic compared with the non-paretic muscles.

(c) US Shear Strain Mapping: We will use the Bimanual Arm Trainer to passively move the shoulder repeatedly into ER at a steady rate set by a metronome (**Figure 9, unimanual mode**). This has the advantage of creating a reproducible rate and amplitude of input motion which is difficult to achieve otherwise. The movement can be performed by moving the trough for one arm which is transduced to the other arm. The subject will be positioned in a seated position as shown in **Figure 9B** so that the infraspinatus muscle is accessible from the back, and the pectoralis major muscle will be accessible from the front. The skin over the muscles will be marked and the transducer will be stabilized so that the tissues are not compressed at any time. Shoulder ER will be performed repeatedly at 0.5 Hz starting from a position of internal rotation with a range of 30° excursion for each cycle. This is ~1/3rd of the full range of motion and will bring the forearm into neutral position. During this motion, we will collect an ultrasound cine-loop, sampled at 1 Hz over a 30 second period also using the scanner system used in Aim 1.

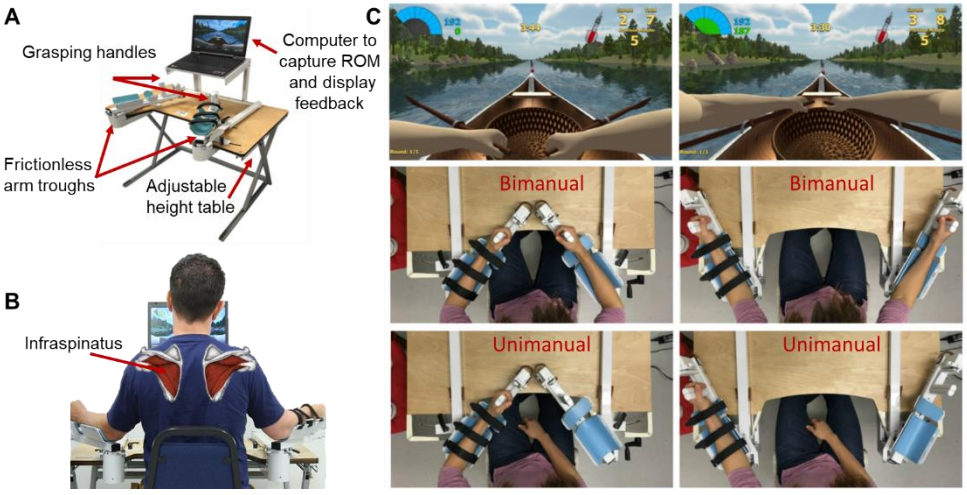

Figure 9. The Bimanual Arm Trainer is an FDA-cleared device that facilitates rate controlled passive shoulder ER-ROM on the paretic side for shear strain mapping, as well as for precise assessment of pain-free shoulder ER-ROM before and after treatment for Aim 3.

US Data Processing: US data acquired from the non-paretic and paretic sides will be processed with a custom program written in Matlab (Natick, MA). Tissue displacements between successive US frames will be estimated from the "raw" US radio frequency (RF) data using cross-correlation techniques [101, 102] with a 1 mm window incremented with a 90% overlap. The term "US frame" refers to the RF data acquired at each time point in the cine-loop. Tissue lateral displacement will be computed for each successive pair of US frames in a 1 × 1.5 cm ROI centered laterally on the midpoint of the image. To visually document the presence of a shear plane within the muscle, we will generate successive displacement maps as a spatial representation of the displacement within the ROI for each pair of US frames. Corresponding cumulative lateral displacement maps will be obtained by summing tissue displacements over time. To calculate the magnitude of shear deformation at a standardized location across subjects, we will use a reference echolucent plane that is relatively stable during the movement and define sub-ROIs each 2 mm × 10 mm for analysis. The maximum shear strain in the sub-ROIs will be averaged and used for statistical analysis.

US Data Analysis: The mean values and standard deviations of the maximum shear strain will be obtained from the defined regions of interest in the pectoralis major and infraspinatus muscles and will be compared for latent and active PSSP on the paretic and non-paretic sides using mixed model analysis, as described above for Aim 1. We will use Pearson's correlations to correlate the clinical and imaging measures.

Expected results, potential pitfalls & solutions: We expect that the mean maximum shear strain will be statistically significant between the healthy (non-paretic) and paretic latent and active PSSP groups to proceed to the R33 phase. We will have twice as much data for the non-paretic arm than for the latent and active PSSP groups. Since some subjects with stroke may not have perfectly healthy non-paretic sides, we will use the data from the healthiest subjects based on their clinical testing, which may provide a greater separation between these groups. ***The quantitative US data will be collected and analyzed in collaboration with Co-I Dr. Muyinatu Bell at Johns Hopkins with Co-I Dr. Siddhartha Sikdar at George Mason University.***

b. Study duration and number of study visits required of research participants.

This study is cross-sectional and will take place over two-years. Each participant will come to the lab for three sessions (for clinical assessment, ultrasound and MRI), each of which will take around 3-4 hours.

c. Definition of treatment failure or participant removal criteria.

Patients will be advised verbally and in the written ICF that they have the right to withdraw from the study at any time without prejudice or loss of benefits to which they are otherwise entitled. The investigator may discontinue a patient from the study in the event of an intercurrent illness, adverse event, and other reasons concerning the health or well-being of the patient, or in the case of lack of cooperation, non-compliance, protocol violation, or other administrative reasons. If a patient does not return for a scheduled visit, every effort will be made to contact the patient/caregiver. Regardless of the circumstance, every effort will be made to document patient outcome. The investigator / study team will inquire about the reason for withdrawal, and follow-up with the patient/ regarding any unresolved adverse events. If the patient withdraws from the study, no further evaluations will be performed and no additional data will be collected, but vital status will be documented at the end of the study period.

d. Description of what happens to participants receiving therapy when study ends or if a participant's participation in the study ends prematurely.

The unique identifier key will be retained and will be destroyed two years after the study ends.

e. If biological materials are involved, please describe all the experimental procedures and analyses in which they will be used.

Not Applicable

5. Inclusion/Exclusion Criteria

Inclusion Criteria

- 18 years or older
- Hemiparesis from Ischemic or Hemorrhagic Stroke
- 4- 180 months post-stroke with Hemiparesis since the incidence and intensity of PSSP
- Show a difference of more than 10 degrees of passive ER-ROM between non-paretic and paretic shoulders with or without pain
- Able to provide informed consent and comply with testing protocols

Exclusion Criteria

- Received treatment for spasticity with Botulinum Toxin or Intrathecal Baclofen within the past three months
- Have another neurologic condition that may affect motor response (e.g. Parkinson's disease, ALS, MS)
- Have a contraindication to MRI (claustrophobia, magnetic pacemakers and clips)
- Have non-musculoskeletal PSSP such as only central pain or chronic regional pain syndrome (CRPS)
- Have a complicated medical condition, or significant injury to either upper limb.

6. Drugs/ Substances/ Devices

a. The rationale for choosing the drug and dose or for choosing the device to be used.

b. Justification and safety information if FDA approved drugs will be administered for non-FDA approved indications or if doses or routes of administration or participant populations are changed.

c. Justification and safety information if non-FDA approved drugs without an IND will be administered.

There is no drug or device intervention in this observational study.

7. Study Statistics

a. Primary outcome variable.

This study has two primary outcomes. The first, which is the primary outcome for AIM 1, is to quantify the extent of HA accumulation using 3-D T1ρ MRI in both arms. The second, which is the primary outcome for AIM 2, is to use Quantitative Shear Stain Mapping to distinguish between latent and active PSSP on the paretic side compared with the non-paretic side.

b. Secondary outcome variables.

For AIM 1, the secondary outcome is the imaging that results from the Quantitative US Statistical Texture Mapping.

c. Statistical plan including sample size justification and interim data analysis.

We determined our sample size for the R61 Phase based on the more stringent sample size requirement for Aim 2, which will compare two independent groups, i.e., patients with latent PSSP vs. patients with active PSSP in the paretic arm. Because Aims 1 and 2 have different measurements, we present our power analysis in terms of standardized effect sizes (Cohen's d), which would be applicable to either measurement (26).

Langevin et al's data on shear strain mapping in patients with and without low back pain (LBP), showed that the shear strain was reduced in the LBP group (56.4% ± 3.1%) compared with the No-LBP group (70.2% ± 3.6%), i.e., an extremely large effect size of 3.8, suggesting that large effect sizes are biologically plausible. The effect sizes in Bishop et al's follow up porcine study (83), showed equally large effect sizes comparing shear strain in control animals versus animals with restricted movement (similar to latent PSSP in our study), versus animals with restricted movement plus injury (similar to active PSSP in our study). We conservatively assume a Cohen's d of 1, which though large is not as large as the cited numbers. To detect a difference between latent PSSP versus active PSSP, a sample size of 17 per group is adequate for statistical significance at the 0.05 level with 80% power. For comparisons between paretic versus non-paretic shoulders, we expect greater power for within-person paired comparisons. However, conservatively assuming no advantage due to within-person correlations, we will also have 80% power to detect differences between latent PSSP versus healthy (non-paretic) shoulders and active PSSP versus healthy shoulders (non-paretic). Since we will be making multiple MRI and US measurements in a population that is disabled and in pain, it is possible that there will be some attrition. Hence accounting for 15% attrition, we will enroll 20 patients per latent PSSP and active PSSP group.

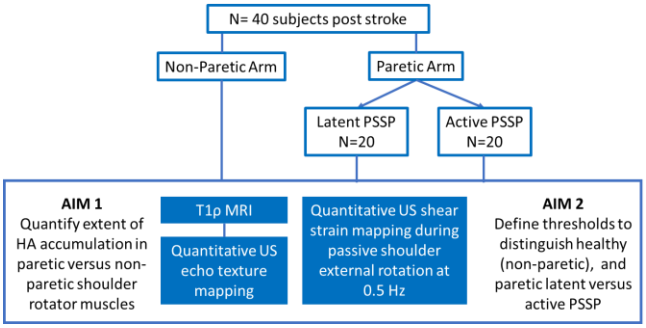

Figure 10. Overview of study design for the R61 Phase.

d. **Early stopping rules**.

Not expected since this is an observational study.

8. Risks

a. Medical risks, listing all procedures, their major and minor risks and expected frequency.

Expected risks to the subject are as follows:

Risks from the clinical assessments: The clinical assessments pose minimal risk. However, stroke patients may fatigue easily. Subjects may experience discomfort when markers are placed on the skin using adhesives. For range of motion assessment, the subjects may develop erythema and skin irritation. These reactions are temporary and will subside in a few hours.

During shear plane motion assessments, the Bimanual Arm Trainer (BAT) will move the arm passively repeatedly through a small range of motion which may feel awkward or uncomfortable for individuals with abnormal muscle tone. Fatigue can also be a factor from sitting at the BAT during the assessments.

Risks from the ultrasound assessments: The placement of the transducer on the skin requires the use of ultrasound gel which may cause minimal discomfort due to the mild cold sensation on the skin. The ultrasound system uses low frequency ultrasound and subjects cannot feel any sensation from the ultrasound transducer.

Risks from the muscle MRI scan: There are no known harmful effects due to exposure to the magnetic field used. Some people may feel confined and experience anxiety in the scanner. The scanner produces tapping sounds during operation, which may reach very loud levels. In extremely rare cases, a magnet can lose its magnetism, in which case cooling fluids may be released noisily through escape valves and may collect in gas form in the scan room. The gas is not harmful in itself as long as fresh air is available. Some individuals may experience muscle twitches or tingling sensations and/or a slight increase in body temperature during some types of scan activity. These are very unlikely under current MRI guidelines.
Incidental findings: The MRI scans are for research purposes only and not directed toward, nor designed for, clinical diagnosis. However, individuals may be concerned about unexpected findings on their scans. The discovery of these abnormalities may lead to feeling anxious and additional tests with costs and risks not covered by this research. There is a risk of injury during MRI if there are metal objects in the body.

Risk from questionnaires: Subjects will be asked to provide information about their self-reported physical and mental well-being. These questions have a small likelihood of low psychological risk if participants are upset by the questions. Their range-of-motion will also be recorded using video. Since patients will be providing information about their medical history and health status, and their movements will be recorded, there is the potential risk of loss of confidentiality.

Risks related to data privacy: Private, identifiable information will be collected. While every reasonable effort will be made to ensure confidentiality of protected and sensitive personal medical information, there is a risk that this confidentiality is compromised, although the study doctors do not expect this to occur.

b. Steps taken to minimize the risks.

Risks from the clinical assessments: During clinical assessments, we will ensure that subjects are given adequate rest breaks to prevent them from becoming fatigued. Each testing session will not last longer than four hours. Discomfort from markers and adhesives will be mitigated by ensuring comfort and using hypoallergenic adhesives that are less likely to cause a skin irritation. If they develop irritation or discomfort from the electrodes or adhesives, they will be offered ice packs for relief of symptoms. Mechanical stops are in place to avoid any abnormal or excessive range of motion of the joints of the arm when moving with the BAT. If the arm position were to ever become uncomfortable the subject can unstrap the paretic arm using the non-paretic arm.

Risks from the ultrasound assessments: No adverse effects have been associated with ultrasound measurements.

Risks from the muscle MRI scan: Standard screening procedures and restricted access minimize the risk associated with MRI. All subjects will be required to fill out a questionnaire indicating if they have any metallic implants prior to entering the scanner for an MRI. All participants will be checked to ensure that no metallic objects remain on their body before entering the magnet room. These include any loose metal snaps, watches, keys, hair pins, electrodes, and hearing aids. Participants with pacemakers or clips will be excluded from the study. During the MRI, the participant will be monitored through a voice box and visually observed using multiple CCD cameras. The greatest risk of the magnetic field is that a metal object could be pulled into the scanner. To reduce this remote risk, everyone near the magnet will remove all metal from their clothing or pockets when in the scanning environment and the door to the scan room will remain closed during the exam. Some people may feel confined and experience anxiety in the scanner. If any problems arise, the scan will be terminated immediately.
Incidental findings: If any incidental abnormalities are found, we will notify subjects and/or their primary physician.

Risk from questionnaires: These questions have a small likelihood of low psychological risk if participants are upset by the questions. The participant does not have to answer any question that they do not wish to.

Risks related to data privacy: All subject information will be coded.

c. Plan for reporting unanticipated problems or study deviations.

Reportable events defined by the JHM IRB will be reported to the IRB using the: "Protocol Event Report" submission or as a written report of the event (including a description of the event with information regarding its fulfillment of the above criteria, follow-up/resolution and need for revision to consent form and/or other study documentation). Copies of each report and documentation of IRB notification and receipt will be kept in the Clinical Investigator's study file.

d. Legal risks such as the risks that would be associated with breach of confidentiality.

We expect minimal risk to confidentiality. Data are coded, and no identifying information will be used in any analyses or publication. The master list containing the link between the data and the identity will be password-protected and kept on computers that are also password protected. All printed health information and study data gathered during performance of the study are kept in locked files, accessible only to study personnel. Electronic data is coded to protect subject identity and stored on password-protected computer workstations. We adhere to all HIPAA privacy rules that affect research protocols.

e. Financial risks to the participants.

There are minimal financial risks to the participant. The risks include lost time from school or work and travel expenses.

9. Benefits

a. Description of the probable benefits for the participant and for society.

The subjects may or may not derive personal benefits from this study. The detailed evaluation procedures will provide insight into mechanisms to further understand myofascial pain in patients post-stroke, and may be applicable to patients with myofascial pain in general.

10. Payment and Remuneration

Transportation to and from the lab will be paid for by the grant, through Uber/Lyft rides or parking passes. Participants will be paid $100 at the completion of the procedures at the end of the study.

11. Costs

This study will be of no cost to the subject or their insurance provider.

12. Transfer of Materials

Transfer of biospecimens from Johns Hopkins to another organization for research purposes and receipt of biospecimens from an outside organization for your research must adhere to JHU policies for material transfer (https://ventures.jhu.edu/faculty-inventors/forms-policies/) and biospecimen transfer (https://hpo.johnshopkins.edu/enterprise/policies/176/39187/policy_39187.pdf?_=0.622324232879).

There will be no transfer of biospecimens.

Please complete this section if your research involves transfer or receipt of biospecimens.

a. Will you **receive** biospecimens from an external entity for this research? [Yes/No].
If "Yes", please confirm you will secure an MTA/research agreement from the appropriate office (JHTV/ORA) prior to transfer.
See: https://ventures.jhu.edu/technology-transfer/material-transfer-agreements/ .

b. Will you **transfer** biospecimens to an external entity as part of this research? [Yes/No]
If "Yes", please address each of the following:
1) Describe the nature of the research collaboration with the external entity and the rationale for the transfer. (Include an explanation of your intellectual contribution to the design of the research study, resulting data and sharing, and participation in the planned publications.)

2) Please confirm you will secure an MTA through the appropriate office (JHTV or ORA) prior to transfer.
(See: https://ventures.jhu.edu/technology-transfer/material-transfer-agreements/.)

3) If the biospecimens you intend to transfer were obtained through clinical or research procedures at Johns Hopkins and "Other" is selected in Item 4, Section 23, please submit the following items in that Section:

a. A pdf version of a completed JHTV Online "Material Transfer Agreement Request Form for Outbound Material" https://ventures.jhu.edu/technology-transfer/material-transfer-agreements/ **OR** a copy of the COEUS PD (Proposal Development Summary).
b. A completed Biospecimen Transfer Information Sheet https://www.hopkinsmedicine.org/institutional_review_board/forms/.
c. A signed and dated "De-identified Human Subject Certification" https://www.hopkinsmedicine.org/institutional_review_board/forms/
d. Approval documents from recipient site, if applicable.
e. Copies of the consent forms associated with the IRB protocols under which the biospecimens were collected, with language appropriate to this transfer highlighted.
f. The name of the specialist you are working with in ORA to complete a contract/MTA.

Please see the following website for more information about transferring human biospecimens to outside entities: https://www.hopkinsmedicine.org/institutional_review_board/news/announcement_transfer_human_biospecimens_outside_entities.html/ .

References

1. McLean, D.E., *Medical complications experienced by a cohort of stroke survivors during inpatient, tertiary-level stroke rehabilitation.* Arch Phys Med Rehabil, 2004. **85**(3): p. 466-9.
2. Bender, L. and K. McKenna, *Hemiplegic shoulder pain: defining the problem and its management.* Disabil Rehabil, 2001. **23**(16): p. 698-705.
3. Ratnasabapathy, Y., et al., *Shoulder pain in people with a stroke: a population-based study.* Clin Rehabil, 2003. **17**(3): p. 304-11.
4. Adey-Wakeling, Z., et al., *Incidence and associations of hemiplegic shoulder pain poststroke: prospective population-based study.* Arch Phys Med Rehabil, 2015. **96**(2): p. 241-247 e1.
5. Adey-Wakeling, Z., et al., *Hemiplegic Shoulder Pain Reduces Quality of Life After Acute Stroke: A Prospective Population-Based Study.* Am J Phys Med Rehabil, 2016. **95**(10): p. 758-63.
6. Paolucci, S., et al., *Prevalence and Time Course of Post-Stroke Pain: A Multicenter Prospective Hospital-Based Study.* Pain Med, 2016. **17**(5): p. 924-30.
7. Lindgren, I., et al., *Shoulder pain after stroke: a prospective population-based study.* Stroke, 2007. **38**(2): p. 343-8.
8. Vasudevan, J.M. and B.J. Browne, *Hemiplegic shoulder pain: an approach to diagnosis and management.* Phys Med Rehabil Clin N Am, 2014. **25**(2): p. 411-37.
9. Gamble, G.E., et al., *Poststroke shoulder pain: a prospective study of the association and risk factors in 152 patients from a consecutive cohort of 205 patients presenting with stroke.* Eur J Pain, 2002. **6**(6): p. 467-74.
10. De Baets, L., et al., *Characteristics of neuromuscular control of the scapula after stroke: a first exploration.* Front Hum Neurosci, 2014. **8**: p. 933.
11. Nadler, M., et al., *Shoulder pain after recent stroke (SPARS): hemiplegic shoulder pain incidence within 72hours post-stroke and 8-10 week follow-up (NCT 02574000).* Physiotherapy, 2020. **107**: p. 142-149.
12. Torres-Parada, M., et al., *Post-stroke shoulder pain subtypes classifying criteria: towards a more specific assessment and improved physical therapeutic care.* Braz J Phys Ther, 2020. **24**(2): p. 124-134.
13. Shah, R.R., et al., *MRI findings in the painful poststroke shoulder.* Stroke, 2008. **39**(6): p. 1808-13.
14. Pratt, R.L., *Hyaluronan and the Fascial Frontier.* Int J Mol Sci, 2021. **22**(13).

15. Infante, J.R., et al., *Phase 1 trials of PEGylated recombinant human hyaluronidase PH20 in patients with advanced solid tumours.* Br J Cancer, 2018. **118**(2): p. 153-161.
16. Fraser, J.R., T.C. Laurent, and U.B. Laurent, *Hyaluronan: its nature, distribution, functions and turnover.* J Intern Med, 1997. **242**(1): p. 27-33.
17. Purslow, P.P., *Muscle fascia and force transmission.* J Bodyw Mov Ther, 2010. **14**(4): p. 411-7.
18. Okita, M., et al., *Effects of reduced joint mobility on sarcomere length, collagen fibril arrangement in the endomysium, and hyaluronan in rat soleus muscle.* J Muscle Res Cell Motil, 2004. **25**(2): p. 159-66.
19. Raghavan, P., et al., *Human Recombinant Hyaluronidase Injections For Upper Limb Muscle Stiffness in Individuals With Cerebral Injury: A Case Series.* EBioMedicine, 2016. **9**: p. 306-313.
20. Stecco, C., et al., *Hyaluronan within fascia in the etiology of myofascial pain.* Surg Radiol Anat, 2011. **33**(10): p. 891-6.
21. Menon, R.G., et al., *T1rho-Mapping for Musculoskeletal Pain Diagnosis: Case Series of Variation of Water Bound Glycosaminoglycans Quantification before and after Fascial Manipulation((R)) in Subjects with Elbow Pain.* Int J Environ Res Public Health, 2020. **17**(3).
22. Menon, R.G., P. Raghavan, and R.R. Regatte, *Quantifying muscle glycosaminoglycan levels in patients with post-stroke muscle stiffness using T1rho MRI.* Sci Rep, 2019. **9**(1): p. 14513.
23. Menon, R.G., P. Raghavan, and R.R. Regatte, *Pilot study quantifying muscle glycosaminoglycan using bi-exponential T1rho mapping in patients with muscle stiffness after stroke.* Sci Rep, 2021. **11**(1): p. 13951.
24. Stecco, A., et al., *Stiffness and echogenicity: Development of a stiffness-echogenicity matrix for clinical problem solving.* Eur J Transl Myol, 2019. **29**(3): p. 8476.
25. Stecco, A., C. Stecco, and P. Raghavan, *Peripheral mechanisms of spasticity and treatment implications.* Current Physical Medicine and Rehabilitation Reports, 2014. **2**(2): p. 121–127
26. Langevin, H.M., et al., *Reduced thoracolumbar fascia shear strain in human chronic low back pain.* BMC Musculoskelet Disord, 2011. **12**: p. 203.
27. Klit, H., N.B. Finnerup, and T.S. Jensen, *Central post-stroke pain: clinical characteristics, pathophysiology, and management.* Lancet Neurol, 2009. **8**(9): p. 857-68.
28. van der Helm, F.C. and G.M. Pronk, *Three-dimensional recording and description of motions of the shoulder mechanism.* J Biomech Eng, 1995. **117**(1): p. 27-40.
29. Rundquist, P.J., et al., *Three-dimensional shoulder complex kinematics in individuals with upper extremity impairment from chronic stroke.* Disabil Rehabil, 2012. **34**(5): p. 402-7.
30. Contemori, S., R. Panichi, and A. Biscarini, *Effects of scapular retraction/protraction position and scapular elevation on shoulder girdle muscle activity during glenohumeral abduction.* Hum Mov Sci, 2019. **64**: p. 55-66.
31. Niessen, M., et al., *Kinematics of the contralateral and ipsilateral shoulder: a possible relationship with post-stroke shoulder pain.* J Rehabil Med, 2008. **40**(6): p. 482-6.
32. Van Ouwenaller, C., P.M. Laplace, and A. Chantraine, *Painful shoulder in hemiplegia.* Arch Phys Med Rehabil, 1986. **67**(1): p. 23-6.
33. Andrews, A.W. and R.W. Bohannon, *Decreased shoulder range of motion on paretic side after stroke.* Phys Ther, 1989. **69**(9): p. 768-72.
34. Bohannon, R.W., et al., *Shoulder pain in hemiplegia: statistical relationship with five variables.* Arch Phys Med Rehabil, 1986. **67**(8): p. 514-6.
35. Zorowitz, R.D., et al., *Shoulder pain and subluxation after stroke: correlation or coincidence?* Am J Occup Ther, 1996. **50**(3): p. 194-201.
36. Braun, R.M., et al., *Surgical treatment of the painful shoulder contracture in the stroke patient.* J Bone Joint Surg Am, 1971. **53**(7): p. 1307-12.
37. Michiels, I. and J. Grevenstein, *Kinematics of shoulder abduction in the scapular plane. On the influence of abduction velocity and external load.* Clin Biomech (Bristol, Avon), 1995. **10**(3): p. 137-143.
38. Ameln, D.J.D., et al., *The Stabilizing Function of Superficial Shoulder Muscles Changes Between Single-Plane Elevation and Reaching Tasks.* IEEE Trans Biomed Eng, 2019. **66**(2): p. 564-572.
39. Hill, A.V., *The mechanics of active muscle.* Proc R Soc Lond B Biol Sci, 1953. **141**(902): p. 104-17.
40. Purslow, P.P. and J.P. Delage, *General anatomy of the muscle fasciae*, in *Fascia: The Tensional Network of the Human Body*. 2012, Churchill Livingstone: London. p. 5–10.
41. Purslow, P.P., *The Structure and Role of Intramuscular Connective Tissue in Muscle Function.* Front Physiol, 2020. **11**: p. 495.
42. Purslow, P.P. and J.A. Trotter, *The morphology and mechanical properties of endomysium in series-fibred muscles: variations with muscle length.* J Muscle Res Cell Motil, 1994. **15**(3): p. 299-308.

43. Passerieux, E., et al., *Physical continuity of the perimysium from myofibers to tendons: involvement in lateral force transmission in skeletal muscle.* J Struct Biol, 2007. **159**(1): p. 19-28.
44. Piehl-Aulin, K., et al., *Hyaluronan in human skeletal muscle of lower extremity: concentration, distribution, and effect of exercise.* J Appl Physiol (1985), 1991. **71**(6): p. 2493-8.
45. Laurent, C., et al., *Localization of hyaluronan in various muscular tissues. A morphological study in the rat.* Cell Tissue Res, 1991. **263**(2): p. 201-5.
46. Laurent, T.C., *Biochemistry of hyaluronan.* Acta Otolaryngol Suppl, 1987. **442**: p. 7-24.
47. Cowman, M.K., M. Hernandez, and J.R. Kim, *Macromolecular Crowding in the Biomatrix.* , in *Structure and function of Biomatrix. Control of Cell Behavior and Gene Expression*, E.A. Balazs, Editor. 2012, Matrix Biology Institute: Edgewater, NJ. p. 45–66.
48. Hascall, V. and J.D. Esko, *Hyaluronan*, in *Essentials of Glycobiology*, A. Varki, et al., Editors. 2015: Cold Spring Harbor (NY).
49. Cowman, M.K., et al., *The Content and Size of Hyaluronan in Biological Fluids and Tissues.* Front Immunol, 2015. **6**: p. 261.
50. Caspersen, M.B., et al., *Thermal degradation and stability of sodium hyaluronate in solid state.* Carbohydr Polym, 2014. **107**: p. 25-30.
51. Cowman, M.K. and S. Matsuoka, *Experimental approaches to hyaluronan structure.* Carbohydr Res, 2005. **340**(5): p. 791-809.
52. Matteini, P., et al., *Structural behavior of highly concentrated hyaluronan.* Biomacromolecules, 2009. **10**(6): p. 1516-22.
53. Snetkov, P., et al., *Hyaluronic Acid: The Influence of Molecular Weight on Structural, Physical, Physico-Chemical, and Degradable Properties of Biopolymer.* Polymers (Basel), 2020. **12**(8).
54. Shimada, E. and G. Matsumura, *Viscosity and molecular weight of hyaluronic acids.* J Biochem, 1975. **78**(3): p. 513-7.
55. Meyer, G.A., A.D. McCulloch, and R.L. Lieber, *A nonlinear model of passive muscle viscosity.* J Biomech Eng, 2011. **133**(9): p. 091007.
56. Elliott, D.M., et al., *Effect of altered matrix proteins on quasilinear viscoelastic properties in transgenic mouse tail tendons.* Ann Biomed Eng, 2003. **31**(5): p. 599-605.
57. Pedrosa-Domellof, F., S. Hellstrom, and L.E. Thornell, *Hyaluronan in human and rat muscle spindles.* Histochem Cell Biol, 1998. **110**(2): p. 179-82.
58. Fukami, Y., *Studies of capsule and capsular space of cat muscle spindles.* J Physiol, 1986. **376**: p. 281-97.
59. Song, Z., R.W. Banks, and G.S. Bewick, *Modelling the mechanoreceptor's dynamic behaviour.* J Anat, 2015. **227**(2): p. 243-54.
60. Edin, B.B. and A.B. Vallbo, *Stretch sensitization of human muscle spindles.* J Physiol, 1988. **400**: p. 101-11.
61. Menon, R.G., P. Raghavan, and R.R. Regatte, *Quantifying muscle glycosaminoglycan levels in patients with post-stroke muscle stiffness using T(1ρ) MRI.* Sci Rep, 2019. **9**(1): p. 14513.
62. Calve, S., et al., *Hyaluronic acid, HAS1, and HAS2 are significantly upregulated during muscle hypertrophy.* Am J Physiol Cell Physiol, 2012. **303**(5): p. C577-88.
63. Laurent, T.C., U.B. Laurent, and J.R. Fraser, *Serum hyaluronan as a disease marker.* Ann Med, 1996. **28**(3): p. 241-53.
64. Naredo, A.E., et al., *A comparative study of ultrasonography with magnetic resonance imaging in patients with painful shoulder.* J Clin Rheumatol, 1999. **5**(4): p. 184-92.
65. Ozcakar, L., et al., *Ultrasound imaging for sarcopenia, spasticity and painful muscle syndromes.* Curr Opin Support Palliat Care, 2018. **12**(3): p. 373-381.
66. Sikdar, S., et al., *Assessment of myofascial trigger points (MTrPs): a new application of ultrasound imaging and vibration sonoelastography.* Annu Int Conf IEEE Eng Med Biol Soc, 2008. **2008**: p. 5585-8.
67. Pavan, P.G., et al., *Painful connections: densification versus fibrosis of fascia.* Curr Pain Headache Rep, 2014. **18**(8): p. 441.
68. Heckmatt, J.Z., S. Leeman, and V. Dubowitz, *Ultrasound imaging in the diagnosis of muscle disease.* J Pediatr, 1982. **101**(5): p. 656-60.
69. Sikdar, S., et al., *Quantification of Muscle Tissue Properties by Modeling the Statistics of Ultrasound Image Intensities Using a Mixture of Gamma Distributions in Children With and Without Cerebral Palsy.* J Ultrasound Med, 2018. **37**(9): p. 2157-2169.
70. Destrempes, F. and G. Cloutier, *A critical review and uniformized representation of statistical distributions modeling the ultrasound echo envelope.* Ultrasound Med Biol, 2010. **36**(7): p. 1037-51.

71. Destrempes, F., et al., *Unifying Concepts of Statistical and Spectral Quantitative Ultrasound Techniques.* IEEE Trans Med Imaging, 2016. **35**(2): p. 488-500.
72. Bureau, N.J., et al., *Diagnostic Accuracy of Echo Envelope Statistical Modeling Compared to B-Mode and Power Doppler Ultrasound Imaging in Patients With Clinically Diagnosed Lateral Epicondylosis of the Elbow.* J Ultrasound Med, 2019. **38**(10): p. 2631-2641.
73. Zhang, Q., et al., *Incidence and Prevalence of Poststroke Shoulder Pain Among Different Regions of the World: A Systematic Review and Meta-Analysis.* Front Neurol, 2021. **12**: p. 724281.
74. Ada, L.P., et al., *Profile of upper limb recovery and development of secondary impairments in patients after stroke with a disabled upper limb: An observational study.* Physiother Theory Pract, 2020. **36**(1): p. 196-202.
75. Flores, D.V., et al., *MR Imaging of Muscle Trauma: Anatomy, Biomechanics, Pathophysiology, and Imaging Appearance.* Radiographics, 2018. **38**(1): p. 124-148.
76. Speer, K.P., J. Lohnes, and W.E. Garrett, Jr., *Radiographic imaging of muscle strain injury.* Am J Sports Med, 1993. **21**(1): p. 89-95; discussion 96.
77. Wilder, R.P. and S. Sethi, *Overuse injuries: tendinopathies, stress fractures, compartment syndrome, and shin splints.* Clin Sports Med, 2004. **23**(1): p. 55-81, vi.
78. Hooijmans, M.T., et al., *Quantitative MRI Reveals Microstructural Changes in the Upper Leg Muscles After Running a Marathon.* J Magn Reson Imaging, 2020. **52**(2): p. 407-417.
79. Bishop, J.H., et al., *Ultrasound Evaluation of the Combined Effects of Thoracolumbar Fascia Injury and Movement Restriction in a Porcine Model.* PLoS One, 2016. **11**(1): p. e0147393.
80. Raghavan, P., et al., *Coupled Bimanual Training Using a Non-Powered Device for Individuals with Severe Hemiparesis: A Pilot Study.* Int J Phys Med Rehabil, 2017. **5**(3).
81. Rajaratnam, B.S., et al., *Predictability of simple clinical tests to identify shoulder pain after stroke.* Arch Phys Med Rehabil, 2007. **88**(8): p. 1016-21.
82. Raghavan, P., et al., *Coupled bimanual training using a non-powered device for individuals with severe hemiparesis: A pilot study.* Int J Phys Med Rehabil 2017. **5**(404).
83. *trackSTAR2 Manual*. 2011; Available from: http://www.ndigital.com/medical/products/3d-guidance/#3d-guidance-technical-specifications.
84. Bohannon, R.W. and M.B. Smith, *Interrater reliability of a modified Ashworth scale of muscle spasticity.* Phys Ther, 1987. **67**(2): p. 206-7.
85. Gilman, S., *Joint position sense and vibration sense: anatomical organisation and assessment.* J Neurol Neurosurg Psychiatry, 2002. **73**(5): p. 473-7.
86. Treede, R.D., et al., *A classification of chronic pain for ICD-11.* Pain, 2015. **156**(6): p. 1003-1007.
87. Rolke, R., et al., *Quantitative sensory testing: a comprehensive protocol for clinical trials.* Eur J Pain, 2006. **10**(1): p. 77-88.
88. Krause, T., et al., *Chronic sensory stroke with and without central pain is associated with bilaterally distributed sensory abnormalities as detected by quantitative sensory testing.* Pain, 2016. **157**(1): p. 194-202.
89. Chae, J., *Poststroke complex regional pain syndrome.* Top Stroke Rehabil, 2010. **17**(3): p. 151-62.
90. Niehof, S.P., et al., *Thermography imaging during static and controlled thermoregulation in complex regional pain syndrome type 1: diagnostic value and involvement of the central sympathetic system.* Biomed Eng Online, 2006. **5**: p. 30.
91. Fugl-Meyer, A.R., et al., *The post-stroke hemiplegic patient. 1. a method for evaluation of physical performance.* Scand J Rehabil Med, 1975. **7**(1): p. 13-31.
92. Wolf, S.L., et al., *Assessing Wolf motor function test as outcome measure for research in patients after stroke.* Stroke, 2001. **32**(7): p. 1635-9.
93. Bogard, K., et al., *Can the Wolf Motor Function Test be streamlined?* Neurorehabil Neural Repair, 2009. **23**(5): p. 422-8.
94. Chen, H.F., et al., *Rasch validation of the streamlined Wolf Motor Function Test in people with chronic stroke and subacute stroke.* Phys Ther, 2012. **92**(8): p. 1017-26.
95. Duncan, P.W., et al., *Stroke Impact Scale-16: A brief assessment of physical function.* Neurology, 2003. **60**(2): p. 291-6.
96. Lai, S.M., et al., *Physical and social functioning after stroke: comparison of the Stroke Impact Scale and Short Form-36.* Stroke, 2003. **34**(2): p. 488-93.
97. Kroenke, K., R.L. Spitzer, and J.B. Williams, *The PHQ-9: validity of a brief depression severity measure.* J Gen Intern Med, 2001. **16**(9): p. 606-13.

98. Mitrea, B.G., et al., *Paired self-compensated spin-lock preparation for improved T1rho quantification.* J Magn Reson, 2016. **268**: p. 49-57.
99. Dixon, W.T., *Simple proton spectroscopic imaging.* Radiology, 1984. **153**(1): p. 189-94.
100. Reeder, S.B., et al., *Iterative decomposition of water and fat with echo asymmetry and least-squares estimation (IDEAL): application with fast spin-echo imaging.* Magn Reson Med, 2005. **54**(3): p. 636-44.
101. Ophir, J., et al., *Elastography: a quantitative method for imaging the elasticity of biological tissues.* Ultrason Imaging, 1991. **13**(2): p. 111-34.
102. Konofagou, E. and J. Ophir, *A new elastographic method for estimation and imaging of lateral displacements, lateral strains, corrected axial strains and Poisson's ratios in tissues.* Ultrasound Med Biol, 1998. **24**(8): p. 1183-99.